Flow Study in the Lantau Island of Hong Kong

Kin-Sang Chim*, Kai-Hon Lau*, See-Chun Kot**, Jay-Chun Chen*
*CCAR, **Mechanical Engineering Department,
Hong Kong University of Science and Technology

Corresponding Author : Kin-Sang Chim
Email : chimkinsang@hotmail.com
: mecks@ust.hk
Tel : (852) 2358 6925

Abstract

The two highest peaks of Lantau Island are the Lantau Peak and Sunset Peak which height attains 934m and 869m respectively. Lantau Island located in the Southwestern part of Hong Kong where the left hand side is the Pearl River Estuary and to the East is the Hong Kong Island. The southern part of Lantau island is face to the South-China Sea. Castle peaks and Tuen Mun located in the northern side of the Lantau Island. The East-West dimension of Lantau Island is about 20km and the North-South direction is in the scale of 13km. It is a typical Meso-Gamma Scale domain. Between these two hill peaks, a flow channel is formed in the orientation of Southeast to Northwest direction. The purpose of this study is concern of the topography effect on wind field caused by Lantau Island and the surrounding terrain. Moreover, the Hong Kong Chek Lap Kok International Airport is to the North of Tung Chung. To the north of Airport, TuenMun is in the flow channel formed on the east side by hilly terrain (400m) and the west side by Castle Peak(583m). The wind enhancement by the flow passing this channel will be simulated. The modified PennState/NCAR MM5 model was initialised by the Hong Kong Observatory averaged sounding in order to study the topography effect. A set of numerical experiments is set-up with the topography effect around that region. Firstly, the surrounding topography around Lantau Island will be removed to study solely the topographical effect of the Lantau Island. Secondly, the surrounding topography, include the TuenMun and Castle Peak (583m), will be include in the simulation to study the combination of topographical effect.

Introduction

The major concern of the present study is the topographical effect of the Lantau island on Hong Kong. The topographical effect of both Lantau Island itself and the surrounding terrain will be considered. The general terrain features of the Lantau Island were already mentioned on the abstract. On the other hand, the highest peak of Hong Kong, Tai Mo Shan (957m), is located to the north-east of the Lantau Island, 20 km from Tung Chung. To the north of Tung Chung, 8km, the Castle Peak (583m) and the Tuen Mun area form a typical flow channel. To the south and west of Lantau Island, there are a few small islands with maximum terrain height of 300m. From the simulation of the present study, those small islands have minimal effect on the surface flow pattern. It is speculated that the temperature change of sea surface temperature to the south or west of Lantau Island would be more important on the surface wind field when compared to the topographical effect of those small island. But the effect of variation of the sea surface temperature is beyond the scope of the present study. All simulations in the present study will assume a constant value for the sea surface temperature.

This paper contains five sections. After the introduction, the model setup and the discussion of the numerical experiments are followed. In the third and fourth sections the numerical simulations with and without the surrounding Tuen Mun terrain respectively will be presented. The fifth section is the conclusions.

Model Setup and Numerical Experiments

The PennState/NCAR MM5 model is used in the present study. The model is modified so that it can handle the upper boundary energy reflection of vertically propagating wave by Klemp and Lilly (1978) upper dissipative layers. Moreover, Orlanski(1976) open lateral boundary condition are also implemented.

The model is initialised by the single sounding initialisation method, Chim (1997). That means only single vertical profile of wind data are required to initial the model.

Physical options that are used for the simulations are Bulk-Aerodynamic PBL Deardroff(1972) with surface heat fluxes and surface moisture fluxes being turn off. Moreover, potential temperature is used in the advective and adiabatic term rather than using the traditional temperature. The ground and sea surface temperatures are kept constant during the integration.

On the other hand, physical options that are not used include the Cumulus parameterization and the Coriolis effect because of the small scale of the computational domain.

The computational domain is spanned by 91 * 91 grids on horizontal plane with grid size equal to 667m. Sigma coordinate is used to define the vertical layers of the model and there are 27 half-sigma levels in the vertical axis. In order to satisfy the CFL condition, the model uses 2 seconds as its time step. The total integration time is designed to be 180 minutes. That is due to two factors, the first one is based on the past experience that the model will attain the steady state after 5100 seconds which are equal to 85 minutes. We take 180 minutes so that the model has more than double the integration time for the flow to be steady. The second reason is that the model should provide enough time so that the air parcels can advected from one side of the domain to the opposite side of the domain. Consider the typical wind speed of 5~6 m/s, for 91 grids, it takes about 180 minutes for the air parcel to advect from one side to the other side of the computational domain.

The paper contains a set of four numerical experiments. The numerical experiments setup is defined as Table. 1.

Table.1

EXP1	EXP2	EXP3	EXP4
HKO 1991 July average sounding	HKO 1991 October average sounding	HKO 1991 July average sounding	HKO 1991 October average sounding
Excluded TuenMun	Excluded TuenMun	Included TuenMun	Included TuenMun

The first two experiments EXP1 and EXP2 are designed to investigate the topographical effect on wind field by the Lantau Island. The EXP3 and EXP4 include the Tuen Mun terrain in the computational domain to investigate the combined topographical effect on wind field by Lantau Island and the surrounding topography. In the second row of Table.1, HKO stands for the Hong Kong Observatory and 1991 average sounding denotes the average sounding that was released by HKO for year 1991, "Summary of Radiosonde-Radiowins Ascents made in 1991". Fig.1 and Fig.2 show the skew-T plot of the 1991 average sounding for July and October respectively. The third row of Table.1 denote the terrain data that are used, which have two configurations, one include the TuenMun and the surrounding terrain and the other excludes those terrain.

Simulation without TuenMun

Fig.3 shows the wind field at 995mbar level for EXP1. In order to have a clearer illustration, the wind arrows in Fig.3 are enhanced by the scale factor of 5. Moreover, as the computational domain is very small when compare to the traditional Mesoscale simulation, grid number is used to replace the Latitude and Longitude to specify the location. The EXP1 uses 1991 July average sounding, so that the surface flow has a Froude number of 0.25. This is in the Splitting Flow Regime as defined by Miranda and James (1992). According to the sounding data, the wind at 1000 mbar level is 2 m/s while at 800 mbar level, the wind is 10 m/s.

In this simulation, flow stagnation is found at the grid number (45,23) where the first number denotes the x-axis index while the second one is the y-axis index. Moreover, wind speed enhancement is found on the northern side of Lantau Island, especially the Tung Chung (40,40), Sham Wat (32,38) and Pak Mong (46,42) area with maximum wind enhancement of 2.85 times. Maximum wind speed that is simulated attains 5.7 m/s at Sham Wat.

Unlike the traditional theory for low Froude number flow across idealized obstacle which predicts stagnation existing both in the windward side and the lee side of the obstacle. The simulation only predicts stagnation in the windward side, however, the wind speed in the lee side has more than 2 times of enhancement.

Fig.4 is a vertical cross section YCUT55, parallel to x-axis at grid number 55, of the wind field up to 3 km height of EXP1. In order to show the surface values clearly, the figure is plotted such that the terrain data is a little bit lower than the actual ground level and which is mark by 0 in the vertical coordinate.

The continuous lines are the isentropes in $0.5^{\circ}K$ interval. This figure is plotted such that the wind is blowing into the paper. A pair of counter-rotating vortices is observed in the grid number 31 and 45. The mean two dimensional wind speed at surface layer in this cross-sectional plane is 0.5 m/s which is only _ of the mean three dimensional wind speed. That means the flow into the paper is the dominant property, and those pair of counter rotating vortices is only a secondary property in this plane. Thus the topographical effect is only a minor contributor to the vertical mixing in this simulation.

EXP2 represents the simulation initialised by the averaged October sounding of year 1991. For this particular sounding, wind magnitude in lower level varies from 2 m/s at the ground to 4 m/s at 800 mbar level. Moreover, the Froude number varies from 0.19 to 0.25 and is also within the Splitting Flow Regime. Fig.5 denotes the streamline of the EXP2 simulation. The recirculation is simulated behind Lantau , noting the northery wind for this case. Moreover, a very small recirculation is found on the Cheung Sha, grid number (42,27). The typical low-froude number flow characteristic such as windward side stagnation, lee side stagnation and lee side recirculation are also simulated in this experiment.

Simulation with TuenMun

Fig.6 denotes the wind arrow plot of EXP3 at 995 mbar level. Unlike the EXP1 which neglects the topography of the TuenMun(45,57) area, a local stagnation occur to the north-east of Tung Chung, 4km away. Moreover, to the south of TuenMun area, the wind speed attains 6.5 m/s at grid (42,52) and which is 14% larger than the maximum wind magnitude that EXP1 predicts. For EXP3, in the vertical cross-section YCUT55, a pair of vortices is also simulated but this time the vortices are circulating in the same clockwise sense, the figure is not shown.

Fig.7 is the streamline plot of EXP4. Wind comes from 4°, from north to south. In the lee side of Lantau island, a pair of lee vortices is identified, grid number (32,25) and (50,25). Another vortex is found on Tsing Yi (63,44). It is speculated that this kind of atmospheric structure favours the air pollutant cumulated in this area and raises the air pollution index in this area subsequently. Moreover, lee side stagnation is found on grid number (44,7). In order to discuss this simulation more precisely, the wind arrow plot is provided in Fig.8. The wind arrows in Fig.8 are scaled by a factor of 5. Maximum wind magnitude is found on grid (42,53) and it is 3 times larger than the initial sounding value at the same level. This flow enhancement area is located just on the lee side of the TuenMun flow channel.

Fig.9 is the vertical cross-section XCUT42 parallel to y-axis and cut at grid number 42. This cross-section is cut right through the plane where maximum wind enhancement is simulated at the lee side of the TuenMun channel. In the figure, air flow from right to left, targeting on surface flow there is a stagnation region in the surface layer at grid 75 which is upstream of the TuenMun terrain when compare to Fig.7 the flow splits and flows around the terrain. The maximum wind enhancement occurs at grid number 52. Stagnation point exists again at grid number 43, here the flow splits around the Lantau Island and flow reversal is predicted in the lee side of the Lantau Island, from grid 8 to grid 31. By using the idea of low-Froude number flow over a Gaussian obstacle, the stagnation occur at grid 75, grid 52 and grid 8 can be explained by the theory. The wind magnitude enhancement at grid 52 is not the characteristic of the low Froude number flow over obstacle. It is speculated that it is caused by the channel effect from the flow across the TuenMun channel.

Fig.10 shows the vertical cross-section YCUT25. The contours are the isentropes in $0.5^{\circ}K$ increment and wind arrows are enhanced by the scale factor of 5. This cross-section cut right across those two lee side vortices with vortex center at grid 32 and grid 50. A downwash is simulated in both of the grid locations. This kind of downwash in company with the lee side vortices is important for air pollution study. As not only pollutants in the surface layer will accumulated in the centre of lee vortices, but the pollutant accumulated in the 1~2km level above ground will be draw down by the wind flow to the ground level by this kind of atmospheric phenomenon.

Conclusion

The Hong Kong Observatory 1991 July and October averaged soundings are used to study the topographical effect of Lantau Island and the surrounding terrain. For the July simulation without the TuenMun topography, stagnations found to the south of the Cheung Sha, but unlike the typical low-Froude number flow around an idealized obstacle, there is no stagnation at the downstream side. At the

downstream side of Lantau Island, there exists a 2.85 times of wind speed enhancement at Tung Chung, Sham Wat and Pak Mong areas. Moreover, lee side counter-rotating horizontally oriented vortices are simulated. But the vertical motion of these vortices is not enough to bring the air parcel from 1-2km about ground level into the surface layer. For the upstream simulation with TuenMun topography, 5km to the east of the TuenMun, the simulated wind magnitude is 14% larger than the simulation without TuenMun terrain.

For the October simulation without TuenMun topography (EXP2), all the flow characteristics of low-Froude number flow are simulated. The simulations with the TuenMun topography (EXP4) show the existence of lee side vortices to the south of Lantau Island. The vertical cross-sectional cut at the centre of the lee side vortices show that there is downwash in the centre of lee side vortices. This atmospheric phenomenon is believed to be responsible for drawing the pollutants originally in the 1-2km above sea level down to the surface layer. But this is only a single case study, more research have to be performed to verify this point. Moreover, in the lee side of TuenMun flow channel, 3 times wind enhancement with related to the initial sounding are found. Moreover, vortex is also found on the Tsing Yi island which implies that this is the place to have more chances of observing high air pollution index.

The present study uses the Hong Kong Observatory averaged sounding to initialise the modified version of the PennState/NCAR MM5 model. As the sounding is not a real sounding, there is no comparison between the observation and the model simulation.

Reference

Chim Kin-Sang., Kai-Hon Lau., See-Chun Kot., 1997:
"Single sounding Initialization of Micro-Alpha Scale Flow over Complex Terrain Using the Penn State/NCAR MM5 Model". Proceeding of The Seventh PSU/NCAR Mesoscale Model Users' Workshop. NCAR, Boulder, Colorado, USA 40-44.

Deardorff James. W., 1972:
Parameterization of the Planetary Boundary Layer for Use in a General Circulation Models. Monthly Weather Review. Vol 100, No.2, 93-105.

Klemp. J.B., and D. K. Lilly., 1978:
Numerical Simulation of Hydrostatic Mountain Waves. Journal of the Atmospheric Sciences. Vol 35. 78-107.

Miranda, P.M.A., and I.N.James., 1992:
Non-Linear three dimensional effects on gravity-wave drag: Splitting flow and breaking waves. Q.J.R Meteorol. Soc. 1057-1081.

Orlanski, I., 1976:
A Simple Boundary Condition for Unbounded Hyperbolic Flows. Journal of Computational Physics, 21. 251-269

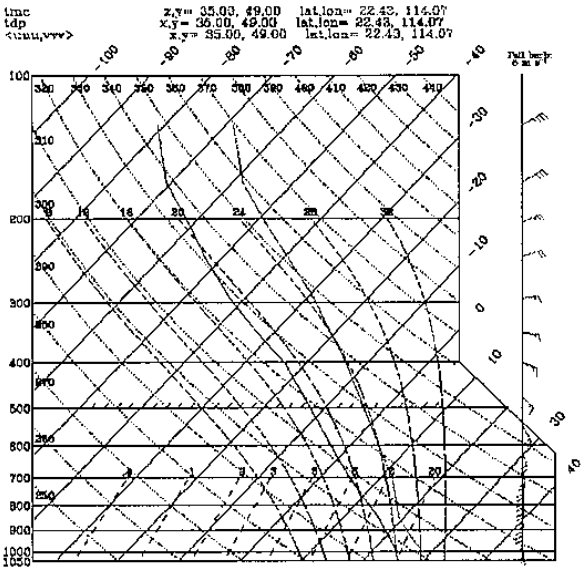

Fig.1 Skew-t plot of HKO 1991 July averaged sounding.

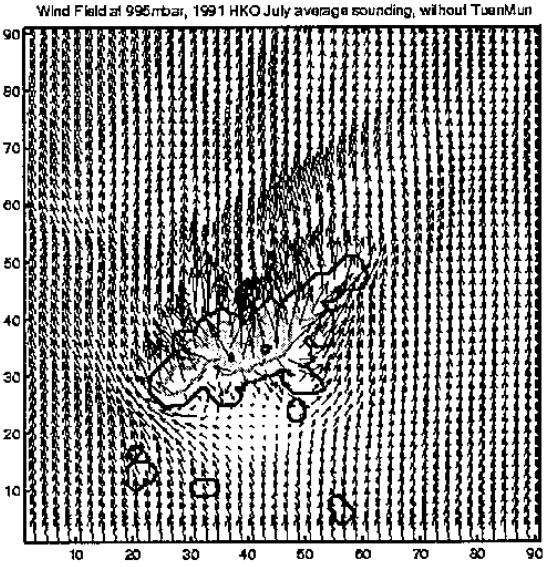

Fig.3 Wind arrow at 995mbar of EXP1, HKO 1991 July averaged sounding. Wind arrows scaled by factor of 5.

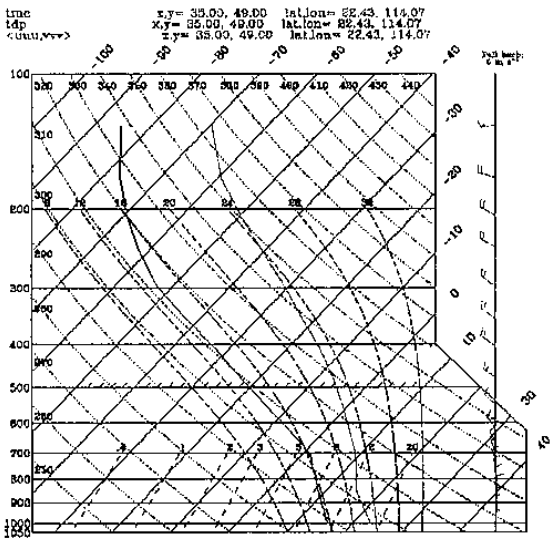

Fig.2 Skew-t plot of HKO 1991 October averaged sounding.

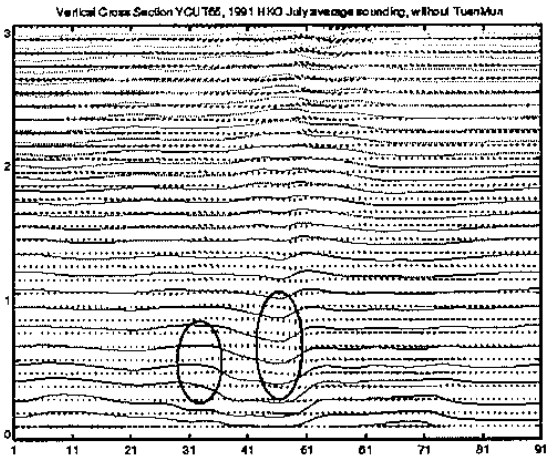

Fig.4 Vertical cross section YCUT55 of EXP1, contour line denotes the isentropes in $0.5^{\circ}K$ contour interval.

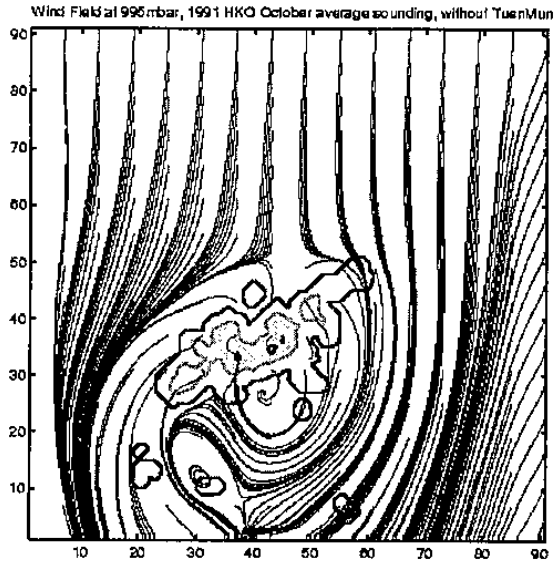

Fig.5 Streamline at 995mbar of EXP2

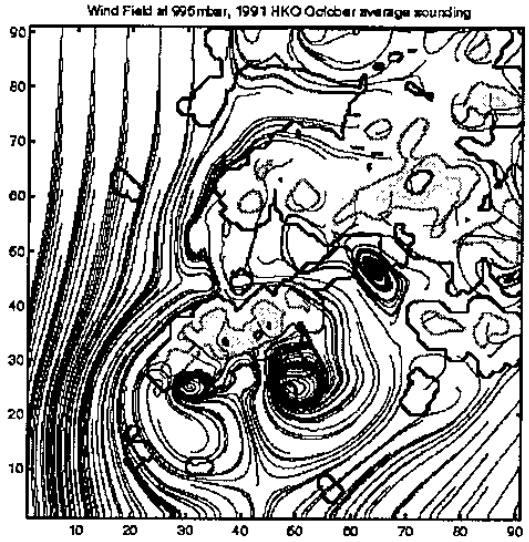

Fig.7 Streamline of 995mbar of EXP4

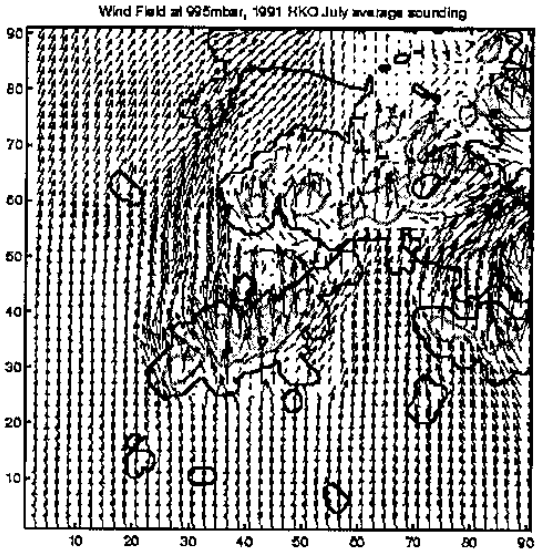

Fig.6 Wind Arrows at 995mbar of EXP3, wind arrows scale by factor of 5.

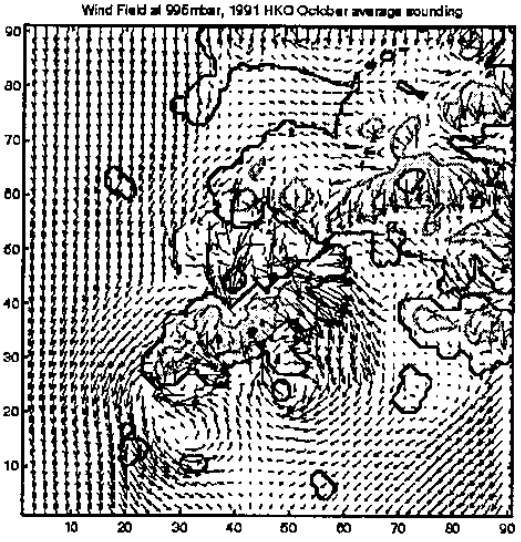

Fig.8 Wind arrows at 995mbar of EXP4, wind arrows scaled by 5.

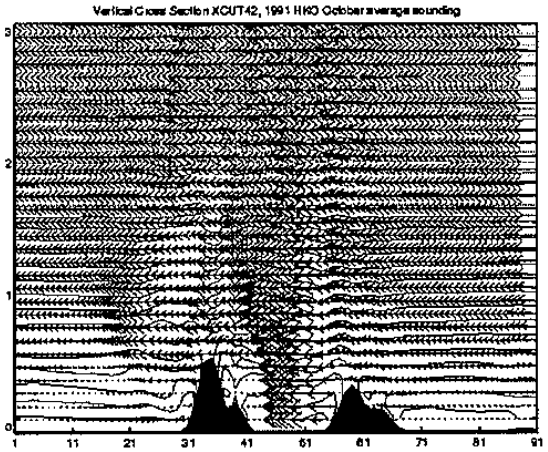

Fig.9 Vertical cross section XCUT42 of EXP4. Wind arrows scaled by 5. Thin continuous denotes isentropes in 0.5℃ contour interval.

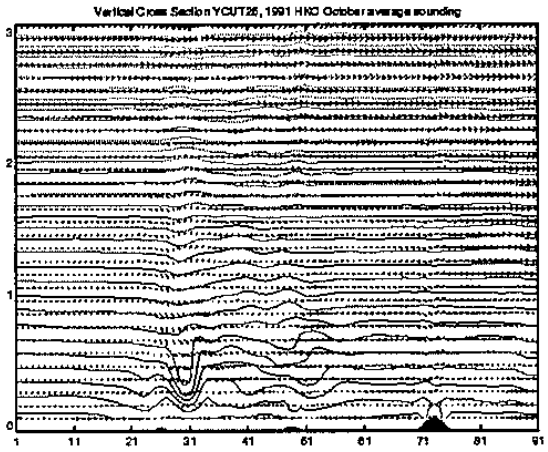

Fig.10 Vertical cross section YCUT25 of EXP4. Wind arrows scaled by 5.